

Optimization of Passenger Car Door Impact Beam using Quasi Static CAE Analysis

S.P. Sundar Singh Sivam^{a,b}, Ganesh Babu Loganathan^c, K. Saravanan^d, V.G. Umasekar^{a,e} and T.P. Mohammed Rameez^{a,f}

^aDept. of Mech. Engg., SRM Institute of Sci. and Tech., Kattankulathur, Tamil Nadu, India

^bCorresponding Author, Email: sundar.sp@ktr.srmuniv.ac.in

^cDept. of Mechatronics Engg., ISHIK University, ERBIL, KRG, Iraq

Email: ganesh.babu@ishik.edu.iq

^dDept. of Mechatronics Engg., SRM University, Kattankulathur, Tamil Nadu, India

Email: saravanan.kn@ktr.srmuniv.ac.in

^eEmail: umasekar.g@ktr.srmuniv.ac.in

^fEmail: mohammedrameeztp@gmail.com

ABSTRACT:

Automotive side impacts are particularly dangerous as location of impact is very close to the passenger, who can be immediately reached by the impacting vehicle. FMVSS 214 static is a US safety regulation for occupant safety during side impacts, in which the vehicle is tested at static loading conditions to measure its load bearing capacity and integrity of side closures. The CAE load case, virtually simulating the test, was handled as a quasi-static problem in this study. Impact beam is a component that helps in improving vehicle passive safety performance during side impacts by minimizing door intrusion to the occupant cabin. It plays an important role in achieving side impact regulatory norms. Through this study, a mass optimized front door impact beam design was developed for a passenger car with the help of CAE simulations; FMVSS 214S regulation norms are met. Component thickness, material and cross section shape were the design variables considered for the study. A methodology to perform the component level simulation of the impact beam loading such that it replicates component behaviour during full vehicle simulation was developed. This has helped in reducing the total problem calculation time in solver. This also has minimized the computational cost for the project. CAE simulations required for the study were done using LS-DYNA. ANSA and PRIMER were used as pre-processors and hyper-graph and meta-post were used for post processing.

KEYWORDS:

Impact beam; Automotive side impact; FMVSS 214 static; Optimization; Quasi-static analysis

CITATION:

S.P.S.S. Sivam, G.B. Loganathan, K. Saravanan, V.G. Umasekar and T.P.M. Rameez. 2019. Optimization of Passenger Car Door Impact Beam using Quasi Static CAE Analysis, *Int. J. Vehicle Structures & Systems*, 11(1), 21-26. doi:10.4273/ijvss.11.1.05.

1. Introduction

Side impact is the second most severe crash scenario after frontal-impact[1]. Risk of injury to inhabitant within the event of aspect impact is significantly higher compared to frontal or rear impact because the energy gripping zones at the front and rear of vehicle is high whereas restricted area is on the market to dissipate the impact energy within the event of aspect impact. In such scenario, strength of side door plays an important role in protecting the occupant. Side door beam in door structure contributes significantly towards the lateral stiffness and plays dominant role in limiting the structural intrusion into passenger compartment [2]. Crashworthiness is the ability of a structure to protect its occupants during an impact. It can also be defined as the ability of the vehicle to absorb energy and to prevent occupant injuries in the event of an accident [3]. This work referred in this paper is intended to develop a mass optimized front door impact beam for a passenger car.

Mass reduction of vehicle structure helps in material cost reduction, improved vehicle performance and improved fuel efficiency. With 75% of fuel consumption relating directly to vehicle weight, the automotive industry can expect an impressive 6 to 8 percent improvement in fuel usage with mere 10% reduction in vehicle weight [5-10].

Federal Motor Vehicle Safety Standard 214 Static (FMVSS 214S) regulation is a US safety regulation for side impact safety. As per the regulation, passenger cars to be sold in the US need to clear the FMVSS 214 static test, in which a plunger of diameter 12 inches is used to apply an intrusion of 18 inches on the vehicle in 120 milliseconds. The loading device would be positioned such that it is at least 5 inches above the bottom edge of the door vertically and is at the middle of door span horizontally. The plunger needs to be at-least 0.5 inches above the bottom edge of window opening. The regulation mandates that any passenger car that is tested should clear the following criteria to pass the test.

- 1) The initial crush resistance shall not be less than 2,250 pounds, with or without seats installed.

- 2) The intermediate crush resistance shall not be less than 3,500 pounds or 4,375 pounds with seats installed.
- 3) The peak crush resistance shall not be less than two times the curb weight of the vehicle or 7,000 pounds, whichever is less. With seats installed, it shall not be less than 3.5 times the curb weight or 12,000 pounds, whichever is less.

The initial crush resistance is the average force required to deform the door through the initial 6 inches of crush. The intermediate crush resistance is the average force required to deform the door through the initial 12 inches of crush. The peak crush resistance will be directly obtained from the plot of load versus displacement since it is the largest force required to deform the door through the entire 18 inches crush distance [4].

In FMVSS 214S test, the criteria are based on the resistive force offered by the vehicle against intrusion. Hooke's law states that the force (F) needed to extend or compress a spring by some distance δ is proportional to that distance. That is

$$F = k \delta \quad (1)$$

or equivalently,

$$k = F/\delta \quad (2)$$

Where, k is a constant factor characteristic of the spring and its stiffness and δ is small compared to the total possible deformation of the spring. Stiffness depends upon material properties and geometry. The stiffness of a structural element of a given material is the product of the material's Young's modulus and the element's second moment of area [6].

2. Baseline model benchmarking

As shown in Fig. 1, the baseline vehicle model was benchmarked for its performance in FMVSS 214 static analysis. The impact beam in the baseline model had a mass of 1.6 kg. It had a C shaped cross section (C1) with the dimensions shown in Table 2. The component had a length of 1011mm and a cross section thickness of 2mm. Material used was hot formed steel and its properties of used for baseline model is given in Table 1. Only parts in the vehicle that might play an active role in the analysis were considered for the problem definition. The vehicle model was constrained in all DOFs' at 4 locations - 2 rear wheel region and 2 on the shotgun. A strip of constrain was provided at the lower body in all DOFs' as shown in Fig. 3. The plunger was positioned at a height of 5 inches from the door base and at the mid pint of door span horizontally. The positioning was as per the guidelines for FMVSS 214 static test procedure. A prescribed motion was defined for the plunger such that it would intrude 18 inches into the vehicle in 120 milliseconds. The plunger was defined as a force transducer to extract the reaction forces it experience.

Table 1: Material properties of hot formed steel

Property	Value
Density	7850 kg/m ³
Young's modulus	210 GPa
Poisson's ratio	0.3
Yield stress	1050 MPa

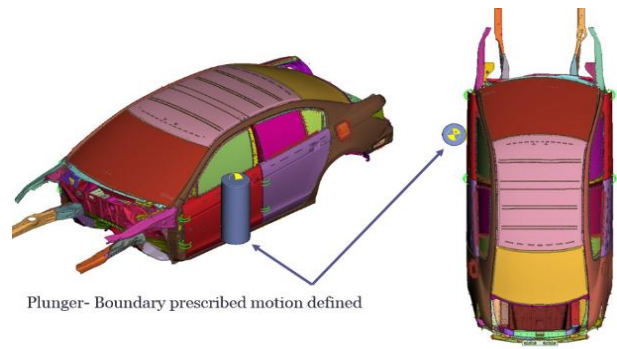


Fig. 1: Baseline vehicle model setup

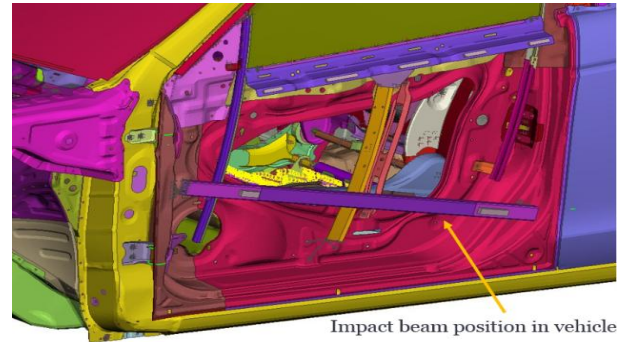


Fig. 2: Impact beam position in vehicle

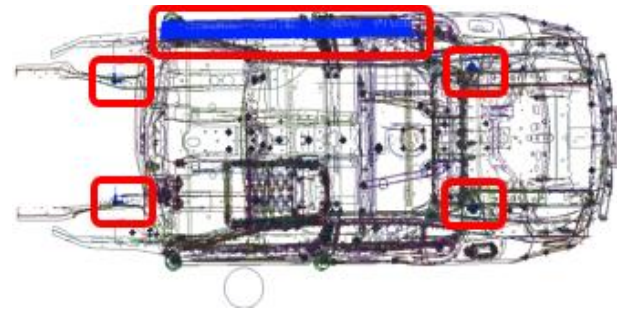


Fig. 3: Constraint positions in vehicle model

Force - Displacement (F-D) plot of the reaction forces acting on plunger was derived by cross plotting Force - Time (F-T) graph from the simulation results and the Displacement - Time (D-T) graph defining plunger motion. From the F-D plot it was evaluated that the plunger offered an initial force resistance of 2830 pounds and an intermediate force resistance of 5980 pounds. The peak force resistance in 18-inch intrusion was 17200 pounds. The baseline model performance is considered to be the benchmark for rest of the study. Optimized component should deliver a performance at least equal to or better than the baseline design during the FMVSS 214 static analysis.

3. Component level test methodology development

Multiple methodologies were evaluated to replicate the component behaviour in vehicle model during a component level simulation setup. Initial considerations for the study were conventional methods like performing the intrusion test with the beam constrained in all DOFs' at both ends as shown in Fig. 4 and 3-point bending test as shown in Fig. 5. These methods were evaluated to be not sufficient for performing an 18-inch intrusion test. In case of beam constrained at both ends, the huge intrusion

would cause component failure, compared to just bending that happens in vehicle model simulation. In a 3-point bending test, poles provided for supporting the impact beam during plunger intrusion was not sufficient to hold the component in position throughout the duration of test as the beam which is of 1011mm length, will pass through the gap between supporting poles after bending during the test. The impact beam was observed to have a partially constrained motion at its ends during the vehicle model simulation, such that its motion is restricted by the stiffness of supporting structures to which the impact beam is attached in the door. From this observation, it was evaluated that providing support to the impact beam at both ends connecting it to a rigid structure with a zero-length spring with a non-linear stiffness in between the impact beam and rigid support would be a possible solution as shown in Fig. 6.

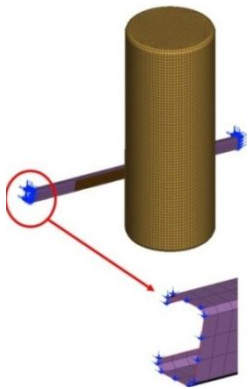


Fig. 4: Component level simulation methodology development - beam constrained in all DOFs at both ends

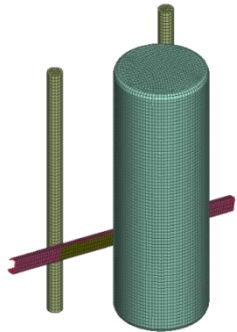


Fig. 5: Component level simulation methodology development - three point bending

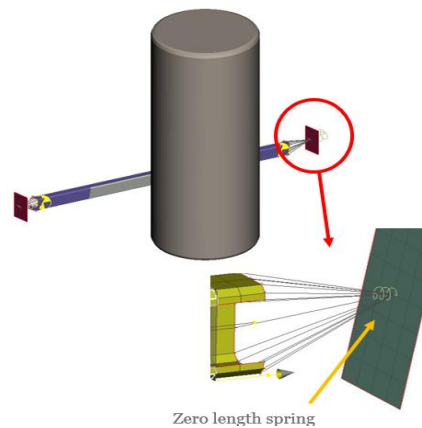


Fig. 6: Component level simulation methodology development - beam constrained at both ends with non-linear springs

The stiffness response of the supporting springs should be similar to the stiffness offered by structures to which the impact beam is mounted in the vehicle. For this, cross sectional forces acting at the front and rear ends of the impact beam were extracted, and based on the intrusion happening at beam ends, F-D curves were plotted for front and rear ends of the impact beam separately. During this process, it was necessary to minimize the effect of external factors on the resistive force response. For this, door outer panel that acts as an intermediate structure between plunger and impact beam, and structures that provide support to the impact beam during intrusion like window glass rail were removed from the model. The portion of beam that comes in contact with plunger was defined as force transducer to measure the force resistance offered by the beam individually as shown in Fig. 7.

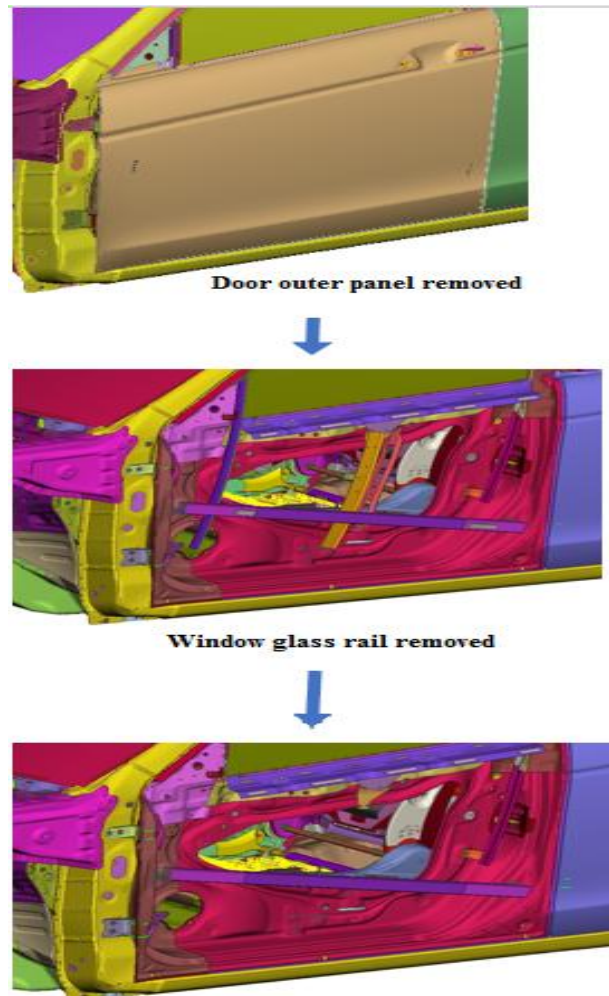


Fig. 7: Modifications made in vehicle model

The F-D response obtained from this transducer that should be matched during the component level analysis. The resistive force acting on plunger involves resistance offered by multiple vehicle structural components. So, it is not sufficient to evaluate resistive force offered by the beam individually. F-D curves plotted for the front and rear ends of the beam in this modified vehicle model were used as F-D curves defining the non-linear response of springs used to constrain the front and rear end of impact beam in component level model. Intrusion analysis performed on this component level simulation

setup gave an F-D plot representing reaction force acting on the impact beam similar to the results obtained from vehicle model modified as in Fig. 7. Based on this observation, the component level simulation setup explained above was used for component level simulations for rest of the simulation iterations.

4. Cross section shape optimization

This stage of optimization aimed at maximizing F-D response of the component during the component level analysis keeping component mass, component length, material and component thickness same as that of baseline model. Maintaining these constraints, 11 design variants with different CS (cross section) shapes were made and evaluated under same component level simulation setup as that of the baseline model. Table 2 shows the design variants studied. Fig. 8 shows the F-D plots comparing best four alternatives identified and baseline model. Table 3 shows the comparison of initial, intermediate and peak intrusion resistance. Based on the evaluation, it was identified that rectangular cross section RC1 delivered the best performance among the cross-sectional shapes analysed.

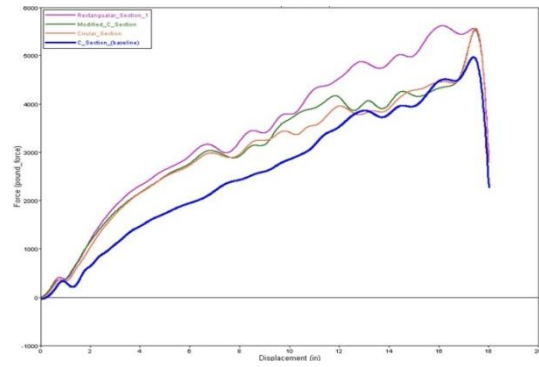


Fig. 8: CS shape optimization- baseline to best three alternative cross section shapes' comparison

Table 3: Performance comparison of baseline to best alternative CS shapes

CS Shape	Initial intrusion resistance (lbf)	Inter. intrusion resistance (lbf)	Peak intrusion resistance (lbf)
C1 (baseline)	1.03E+03	1.85E+03	4.97E+03
C2	1.56E+03	2.48E+03	5.53E+03
O	1.52E+03	2.39E+03	5.56E+03
RC1	1.65E+03	2.62E+03	5.61E+03

Table 2: Cross section shapes analysed

Name	Cross section shape	Name	Cross section shape
C1 (Baseline)		C2	
O		L	
T		I	
M		W	
SQ1		SQ2 (SQ1 orientation changed)	
RC1		RC2	

5. Material selection

Based on material availability and financial feasibility, two different grades of mild steel and an aluminium (Al) alloy were chosen to be evaluated for a performance better than hot formed steel (HFS) which is the baseline material. The grades of mild steel would be referred as “MS-R” and “MS-T”. Properties of the alternative materials are given in Table 4. The shape optimized impact beam, with rectangular (RC1) cross section was analysed at component level simulation setup assigning it with each of the 3 material alternatives. The F-D plot is shown in Fig. 9 and comparing Table 5, the baseline material, hot formed steel, had a superior performance than the available alternatives. Based on this assessment, the study was pursued with no change in material.

Table 4: Material properties comparison

Material	Young’s Modulus (N/m ²)	Density (kg/m ³)	Poisson’s ratio	Yield stress (N/m ²)
HFS	210E+09	7.85E+03	0.3	1050E+06
MS-R	210E+09	7.89E+03	0.3	248E+06
MS-T	207E+09	7.83E+03	0.3	400E+06
Al-alloy	210E+09	7.80E+03	0.3	1000E+06

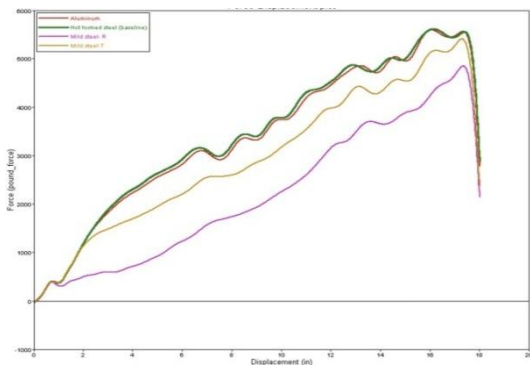


Fig. 9: Material optimization F-D plot

Table 5: Performance comparison - material alternatives

Material	Initial intrusion resistance (lbf)	Inter. intrusion resistance (lbf)	Peak intrusion resistance (lbf)
HFS	1.65E+03	2.62E+03	5.61E+03
MS-R	6.17E+02	1.33E+03	4.85E+03
MS-T	1.30E+03	2.14E+03	5.41E+03
Al-alloy	1.60E+03	2.56E+03	5.59E+03

6. Cross section thickness optimization

The hot formed steel impact beam with rectangular (RC1) cross section delivers a performance much higher compared to that of the baseline design, which has a performance sufficient to clear the FMVSS 214 static regulation. The impact beam was subjected to dichotomous search optimisation, such that the component thickness is minimized with a constraint to maintain optimized component performance greater than or equal to that of the baseline component. The force displacement response of different component thicknesses evaluated is shown in Fig. 10 and Table 6. The component gives a performance closely above the baseline model when its thickness was 1.25 mm.

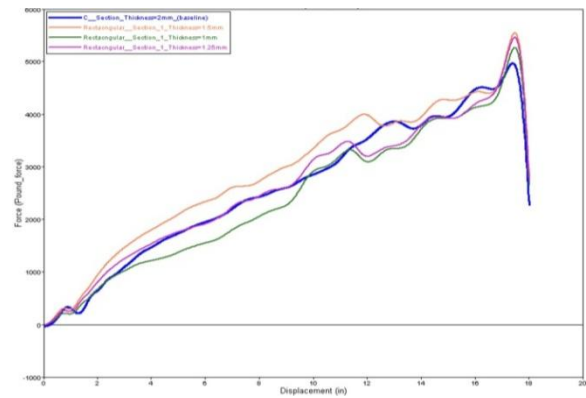


Fig. 10: Thickness optimization F-D plot

Table 6: Performance comparison- Component thickness (in the order of dichotomous search)

CS Thickness	Initial intrusion resistance (lbf)	Inter. intrusion resistance (lbf)	Peak intrusion resistance (lbf)
2 mm	1.03E+03	1.85E+03	4.97E+03
1mm	8.80E+02	1.66E+03	5.26E+03
1.5 mm	1.30E+03	2.20E+03	5.54E+03
1.25 mm	1.10E+03	1.92E+03	5.46E+03

7. Performance evaluation of optimized component in vehicle model

To confirm and evaluate the performance of optimized impact beam in vehicle level, the baseline impact beam was replaced by the optimized one in the baseline vehicle model for analysis. The intrusion resistance performance of the vehicle model with optimized beam and the comparison with baseline vehicle is presented in Fig. 11 and Table 7. The analysis results show that the optimized impact beam has a performance slightly higher than the baseline model and is sufficient to clear FMVSS 214 static regulation.

Table 7: Baseline to optimized vehicle model force- displacement response comparison

Type of Force applied	Vehicle model with baseline impact beam model	Vehicle model with optimized impact beam model
Initial intrusion resistance (lbf)	2.73E+03	2.83E+03
Inter. intrusion resistance (lbf)	5.76E+03	5.98E+03
Peak intrusion resistance (lbf)	1.72E+04	1.79E+04

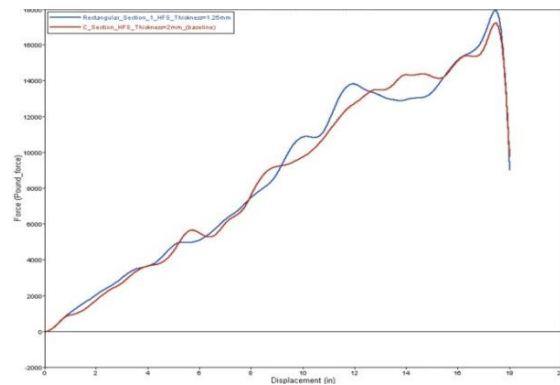


Fig. 11: Baseline to optimized component comparison (vehicle level simulation setup)

8. Evaluation of benefits

Through the study, a reduction of 37.5% was achieved in component mass of front door impact beams (driver and passenger sides). Mass reduction of the component not only brings financial benefits for the automobile manufacturer in terms of material cost, but also helps in achieving improved vehicle performance and fuel efficiency.

9. Conclusion

The study was successful to optimize the mass of impact beam such that the vehicle clears FMVSS 214 static regulation. The study concludes that replacing the baseline model impact beam (C1) with a rectangular cross section impact beam (RC1) can reduce the component mass maintaining intrusion resistance performance of the vehicle above that of baseline model.

ACKNOWLEDGMENT:

I would like to thank Mr. Mrithyunjaya Yeli, Xitadel CAE Technologies, Bangalore for their advice and support. I also thank Mr. Dipu Purushothaman, Fiat Chrysler Automobiles, Chennai for sharing his technical expertise.

REFERENCES:

- [1] *Crashworthiness Evaluation Side Impact Crash Test Protocol (version III)*, Insurance Institute for Highway Safety, April 2004.
- [2] A. Pathak, A. Kumar and R. Lamba. 2017. Effect of beam layout and specification on side door strength of passenger cars: An experimental approach to analyse its effect and contribution to door strength, *SAE Technical Paper*. <https://doi.org/10.4271/2017-26-0023>.
- [3] G.L. Farley and R.M. Jones. 1992. Crushing characteristics of continuous fibre-reinforced composite tubes, *J. Composite Materials*, 26(1), 37-50. <https://doi.org/10.1177/002199839202600103>.
- [4] *Laboratory Test Procedure for FMVSS 214S (Static) Side Impact Protection*. 1992. U.S. Dept. of Transportation, National Highway Traffic Safety Administration.
- [5] S. Ramakrishna and H. Hamada. 1998. Energy absorption characteristics of crashworthy structural composite materials, *Engg. Materials*, 141-143, 585-622. <https://doi.org/10.4028/www.scientific.net/KEM.141-143.585>.
- [6] *Structural Engg. Theory*. 2016. Wikipedia. https://en.wikipedia.org/w/index.php?title=Structural_engineering_theory&oldid=748270532.
- [7] S.P.S.S. Sivam, S.M. Karuppaiah, B.K. Yedida, J.R. Atluri and S. Mathur. 2017. Multi response optimization of setting input variables for getting better product quality in machining of magnesium AM60 by grey relation analysis and ANOVA, *Periodica Polytechnica Mech. Engg.*, 62(2), 118-125. <https://doi.org/10.3311/PPme.11034>.
- [8] S.P.S.S. Sivam, M.D.J. Bhat, S. Natarajan and N. Chauhan. 2018. Analysis of residual stresses, thermal stresses, cutting forces and other output responses of face milling operation on ZE41 magnesium alloy, *Int. J. Modern Manufac. Tech.*, 10(1), 92-101.
- [9] S.P.S.S. Sivam, K. Saravanan, N. Pradeep, K. Moorthy and S. Rajendrakumar. 2018. The grey relational analysis and anova to determine the optimum process parameters for friction stir welding of Ti and Mg alloys, *Periodica Polytechnica Mech. Engg.*, <https://doi.org/10.3311/PPme.12117>
- [10] S.P.S.S. Sivam, V.G. Umasekar, A. Mishra, S. Mishra and A. Mondal. 2016. Orbital cold forming technology - combining high quality forming with cost effectiveness - A review. *Indian J. Sci. and Tech.*, 9(38), 1-7. <https://doi.org/10.17485/ijst/2016/v9i38/91426>.